

“AEROMAGNETIC CONSTRAINTS ON THE STRUCTURAL FRAMEWORK OF UMM FARWAH FAULT SYSTEM AND ASSOCIATED NEOPROTEROZOIC ACCRETION DOMAINS OF THE ASIR TERRANE; THE BILJURSHI AREA, ARABIAN SHIELD”

Taher Zouaghi^{*,1,2}, Essam Aboud^{3,4}, El-Sawy Kamal El-Sawy^{1,5}

⁽¹⁾ Geoexploration Department, Faculty of Earth Sciences, King Abdulaziz University, Jeddah 21589, Saudi Arabia

⁽²⁾ Laboratoire de Géoresources, CERTE, Pôle Technologique de Borj Cédria, Soliman 8020, Tunisia

⁽³⁾ Geohazards Research Center, King Abdulaziz University, Jeddah 21589, Saudi Arabia

⁽⁴⁾ National Research Institute of Astronomy and Geophysics (NRIAG), Helwan, Cairo, Egypt

⁽⁵⁾ Geology Department, Faculty of Science, Al-Azhar University, Assiut, Egypt

Article history

Received November 8, 2018; accepted May 18, 2019.

Subject classification:

Asir terrane, Aeromagnetic, Structural framework, Modeling, Buried geometry.

ABSTRACT

The Arabian Shield and the Pan-African shear zones/terrane boundaries are marked by widespread occurrence of juvenile Neoproterozoic assembly arc terranes. Deep sealed architecture and tectonic framework are still poorly understood because the lack of geophysical studies. N-S oriented lineaments and associated structures that characterize the Asir terrane have crucial interests because they represent the primary constraints to understand structuring and kinematics of the Arabian Shield. The integration of aeromagnetic and geological data of the Biljurshi area highlights the structural setting and its relationship with the Precambrian volcano-sedimentary, metamorphic and plutonic rocks. Results contribute to understand the deep structure of the syn-accretion sedimentary and volcanic system. The geophysical data validate and improve the current geological settings and determine the geometry and tectonic deformation of the Biljurshi subsurface structures. The obtained geometry and structural models will be used to highlight the deep architecture of the Biljurshi area within the Arabian Shield.

1. INTRODUCTION

The Arabian-Nubian Shield (ANS, Figure 1) is a complex interplay between juvenile oceanic and continental arc fragments accreted during the final stages of the Gondwana super continental assemblage [e.g., Collins and Pisarevsky, 2005; Johnson et al., 2011]. It is a conspicuous belt of Precambrian crystalline basement rocks exposed in Northeast Africa and West Arabia as a result of uplift and erosion along the flanks of the Red Sea

[e.g., Genna et al., 2002; Stern, 2002]. The ANS may be the largest tract of juvenile continental crust on Earth [Patchett and Chase, 2002] and is regarded to represent the northern extension of the East African Orogen [EAO; Stern, 1994; Fritz et al., 2013], or the East African–Antarctic Orogen [EAAO; Jacobs and Thomas, 2004] that is now widely considered as a major suture zone separating East and West Gondwana [e.g., Shackleton, 1986, 1994, 1996; Muhongo et al., 2003; Johnson and Woldehaimanot, 2003; Stern and Johnson, 2010].

(less than 740 Ma) [Stoeser and Camp, 1985]. Johnson and Kattan [2001] were separated the Jeddah terrane from the Asir terrane (Figure 1).

The southern part of the Arabian Shield is composed mainly of older (800-1000 Ma) volcanic-arc complex and younger (700-800 Ma) continental marginal (Andean-type) volcanic-arc complex [Prinz, 1983]. These volcanic-arc complexes are located between the more ancient middle Proterozoic continental masses of the west and east Gondwana [Prinz, 1983; Stoeser and Camp, 1985; Meert and Lieberman, 2008; Stern and Johnson, 2010]. North-striking structures of the southern part of the Arabian Shield are related to the accretion phenomenon of late Proterozoic or older arc to the African craton and the subsequent collision of the continental-marginal arc [Prinz, 1983; Stoeser and Camp, 1985; Johnson et al., 1987]. These structures cut across major deposits and appear to have been controlled by the orientation and shape of adjacent continental margins during amalgamation periods [Prinz, 1983]. Amalgamation structures appear to be subduction-related, most of which dipped southwest [Greenwood et al., 1982].

The Ablah marine sedimentary and volcanic molassic syncline (640–615 Ma) [Nehlig et al., 2002; Johnson et al., 2011] is located in the central part of the Neoproterozoic Asir terrane. This post-amalgamation basin contains, around our study area, imprints of terrane accretion composed of volcanic and sedimentary rocks of the Baish, Bahah and Jiddah groups [Greenwood, 1975a; Prinz, 1983] (Figure 2). These groups correspond mainly to the Bidah Belt (~855-815 Ma) to the West, the Shawas Belt (>815 Ma) to the East and the Hali metasedimentary and metavolcanic narrow group/belt (795-780 Ma) to the South [Prinz, 1983; Johnson, 2006]. These belts are marked by Cryogenian intrusive rocks represented by the An Nimas and Buwwah suites and unsigned granite [Greenwood, 1975a; Johnson, 2006].

The Biljurshi area (Figure 2) displays Neoproterozoic typical rocks, namely different types of igneous rocks like diorite/gabbro complexes, and granodiorites [Anderson, 1977; Greenwood et al., 1986]. The Baish, Bahah, and Jiddah Groups were folded, metamorphosed to greenschist facies, and intruded by gabbroic to quartz dioritic plutons about 960 Ma ago during the Aqiq orogeny [Greenwood, 1975a; Prinz, 1983]. Since 800 Ma ago (early phases of the Ranyah orogeny), dioritic to quartz dioritic plutonism recurred [Greenwood, 1975a; Prinz, 1983]. These rock-types are believed to reflect intrusive suites related to intra-oceanic and continental subduction [Anderson, 1977; Greenwood et al., 1986].

The Arabian Shield reveals intra-terrane features that are thought to be a result of major strike-slip and thrust

faulting within the crust. The Umm Farwah dextral slip shear zone [Stoeser and Stacey, 1988; Stern and Johnson, 2010] is one of the main intra-terrane structures of the Asir terrane and is located in the central part of this terrane (Figures 1 and 2). In the Biljurshi study area, the Umm Farwah major fault separates the Baish and Bahah group rocks to the west from Jiddah and Bahah group rocks to the east [Greenwood, 1975a; Prinz, 1983] (Figure 2). Moreover, contrasting metamorphic grades between the two Precambrian rock assemblages were shown along Umm Farwah fault zone [Greenwood, 1975a; Prinz, 1983].

Geochronology data of the Al Qunfudhah quadrangle highlight rocks of Jiddah and Bahah groups, east of the Umm Farwah fault zone, younger than rocks of the Baish and Bahah groups west of the fault zone, although, broadly in the southern part of the Arabian shield, all three groups are essentially contemporary [Greenwood et al., 1982]. At the Asir terrane, Proterozoic rocks west of Umm Farwah fault zone are referred to the Bidah belt, and rocks east of the fault zone are referred to the Tayyah belt [e.g., Prinz, 1983; Genna et al., 2002; Johnson, 2006; Johnson et al., 2013]. The Bidah and Tayyah belts are bounded by similar N- to NE-trending fault zones that represent deep structural breaks in the crust [e.g., Prinz, 1983; Johnson, 2006; Johnson et al., 2013].

The orogenic deposition, deformation, plutonism, and metamorphism observed in the Biljurshi quadrangle are considered to be aspects of the Precambrian Hijaz tectonic cycle that contains three main episodes [e.g., Greenwood, 1975a; Greenwood et al., 1980; Johnson et al., 2003; Al-Shanti, 2009]. The orogenic effects appear to record the formation of continental crust in this area of the Arabian Shield [Greenwood, 1975a; Greenwood et al., 1980; Al-Shanti, 2009]. There is no evidence of an underlying continental basement and the basal units probably were deposited on oceanic crust [Greenwood, 1975a].

The Aqiq orogeny period, belonging to the first episode of the Hijaz cycle, is represented by rocks of the Baish, Bahah, and Jiddah groups that were folded into open to tight north-trending folds with axial plane schistosity, were metamorphosed to greenschist facies, and were intruded by gabbroic to quartz dioritic plutons [e.g., Greenwood, 1975a; Prinz, 1983; Johnson, 2006; Al-Shanti, 2009]. The Ranyah orogeny period, belonging to the second episode of the Hijaz cycle, is represented by Ablah group rocks that are associated with renewed volcanism of andesitic to rhyolitic composition and sedimentation [e.g., Greenwood, 1975a; Greenwood et al., 1980, 1982; Johnson, 2006; Al-Shanti, 2009].

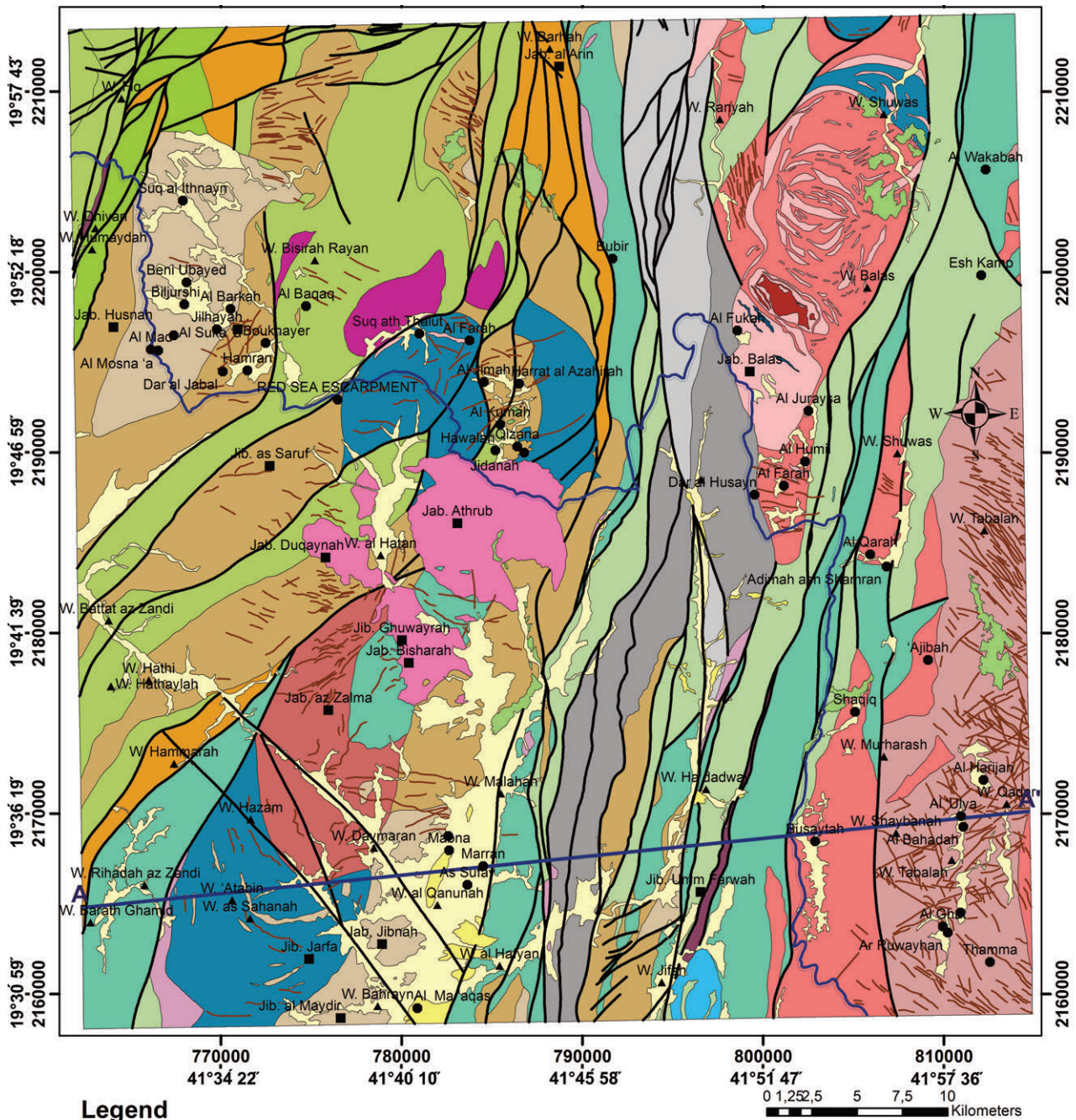


FIGURE 2. Extract of the Biljurshi geological map (1:100 000, resized), showing relation between the Umm Farwah master fault and the associated volcanic, sedimentary and metamorphic rocks and intrusive bodies.

3. DATA AND METHODS

3.1 DATA

The Arabian Shield is covered by regional aeromagnetic surveys. Areas with economic interest were covered by high-resolution aeromagnetic survey. Due to its mining potential, the Biljurshi region was subject of geological and geophysical studies. Aeromagnetic data was acquired during 1966 and 1967. The survey was made by different companies; Lockwood Survey Corp., Ltd.; Aero Service Corp.; Hunting Geology and Geophysics, Ltd.; and the Arabian Geophysical and Surveying Company.

All necessary corrections related to the survey, including diurnal variations, were made by the corresponding companies. The aeromagnetic maps have been interpreted for subsurface features that are often difficult to identify in the field because they are obscured by sedimentary cover and/or by highly weathered rocks. International Geomagnetic Reference Field (IGRF) was removed from the data [Andreasen in Greenwood, 1975a].

The data were acquired along northeast-southwest flight lines spaced 800m, with uniform altitude of 91.5 m above land surface. Because of the high topographic relief in the southwest part of the quadrangle, the aeromagnetic survey was done in two parts delineated approximately by a northwest-southeast diagonal line [Andreasen in Greenwood, 1975a].

3.2 METHODS

The observed magnetic zones reveal a variation of the magnetic field and reflect the distribution of magnetic minerals in the Earth's crust, and thus allow us to detect the deep geological structures [e.g., Jaques et al., 1997; Porwal et al., 2006; Schetselaar and Ryan, 2009]. In this work, various filters, such as reduction to pole (RTP), and horizontal gradient magnitude (HGM), were applied to the magnetic grid to obtain more geophysical information, and thus deduced more geological structures.

The quantitative interpretation of aeromagnetic data aims to infer the parameters in subsurface, such as: the depth, shape, size and magnetic susceptibility of rocks. In this regard, Euler deconvolution and Werner deconvolution are used for depth estimations [Ku and Sharp, 1983; Hinze et al., 2013]. To validate the subsurface sources 2D forward modeling and 3D inversion were applied. The average values used in the modeling were obtained from some confidential report in the Arabian shield, and from the standard charts compiled by various authors [e.g., Clark and Emerson, 1991; Goodwin,

1991; Hunt et al., 1995]. The magnetization vector inversion of the field magnetic data, from induced sources, results in susceptibility contrast in depth.

Remanent magnetization adds more values to measured magnetic field. In the present work, remanent magnetization is assumed negligible, then, all the magnetic responses are related to the induced magnetization of the source. This assumption is taken into consideration to avoid problems of interpretation and especially of the inversion [e.g., Williams, 2008; Cheyney, 2012].

4. RESULTS

4.1 REDUCE TO POLE (RTP)

The Total Magnetic Intensity (TMI) map of the Biljurshi study area ranges from -130 nT to +300 nT (Figure 3A). It shows the difference of high and low magnetic intensity signatures and many crustal magnetization patterns. The magnetic features are differentiated by its intensity, direction, and shape (Figure 3A).

Location of the observed magnetic zones directly above the magnetic causative source bodies requires application of reduced to magnetic pole (RTP) filter to the TMI grid. The TMI grid was transformed into reduction to pole (RTP) by computation of inclination and declination. Inclination of 25.03° and declination of 0.89° were used to generate RTP map. These parameters represent the average value for the Biljurshi area. Both TMI and RTP maps display the major magnetic features. However, RTP shows several significant changes compared to the TMI map (Figure 3B).

The RTP map shows a clear correlation between the high amplitude magnetic zones and the intrusive mafic rocks. It shows that the geological structures are more clearly expressed, for example, the distribution of the meta-volcano-sedimentary structures, the distribution of intrusive igneous rocks and the uplifts of the basement rock. RTP values range from -450 nT to more than +580 nT (Figure 3A). The anomaly pattern can be subdivided into several domains that are superimposed on the different Precambrian rocks. Lithological boundaries are observed from the sharp contrast in the magnetic signature on magnetic sources. Roughly the RTP map shows areas of relatively distinct features that could be classified into five zones of high (H) magnetic intensity values, and four zones of low (L) magnetic intensity values (Figure 3B).

The H1 is the most singular anomaly zone of high magnetic values (Figure 3B). It coincides with geological outcrops of diorite, granite, and associated metagab-

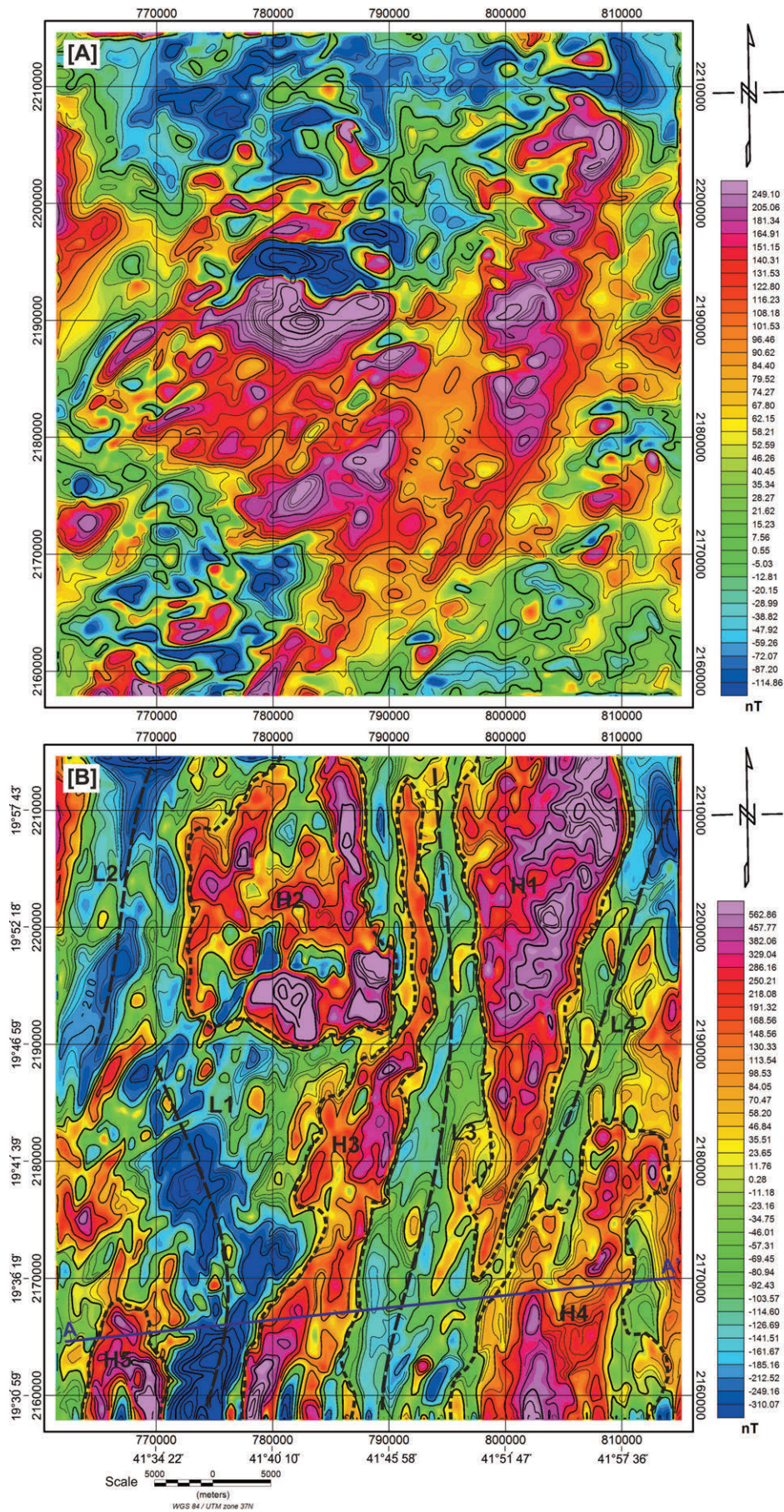


FIGURE 3. Interpretation of reduce to pole anomaly zone map. [A] Total Magnetic Intensity (TMI) map of the Biljurshi study area. [B] Interpreted reduce to pole (RTP) map with location of the studied sections AA'.

bro of the Al Farah–Jabal Balas–Wadi Shuwas region. This zone shows south–north features with a slight deviation towards the northeast in its middle part. The H2 zone covers the area of Jabal al–Arin–Wadi Bisarah Rayan–Al Kumah. It reveals a polygonal–rectangular shape with magnetic features oriented N–S and E–W (Figures 2 and 3B). H2 shows secondary zones of low signatures testifying intense local minima. These secondary shapes coincide with metamorphic and dioritic rocks. The lowest amplitude is recorded at the location of an orthogneiss represented by gray medium–grained granodiorite to quartz monzonitic gneiss [Greenwood, 1975a]. The H3 anomaly zone is located along the western border of the Ablah group belt. RTP map shows linear features of N–S direction to the North, which changed to the south–west in the Wadi Malhah and Jabal Jibnah areas southward. These features of low and high magnetic signatures reflect the deep structure. The intrusive rocks of high magnetic signatures, which constitute the western limit of the Ablah group belt, are interpreted to be intercalated with some other metamorphic and volcano–sedimentary deposits (Figures 2 and 3B). The H4 anomaly zone corresponds to the Busaytah–Ajibah structures that are marked by a portion of N–trending positive feature with a change in orientation of its northern end towards the NNE. This magnetic signature could be correlated with mapped medium–grained hornblende diorite of “Younger Diorite” rocks [Greenwood, 1975a] (Figures 2 and 3B). Offset of the anomaly zones (H1) and (H4) by a zone of NNE– oriented is observed (Figure 3B). The two zones H1 and H4 are linked via a master fault corridor that made a key role in the kinematic evolution of the eastern part of the Biljurshi region and consequently creates a geometric shift (Figure 3B). The fault corridor is associated with exposed bed soles and points of serpentine and talc schist bodies of NNE–SSW direction to the South, and of N–S direction to the North. The H5 zone is superimposed from east to west on the metagabbro of the western part of Jibal Jarfa and granite to granodiorite of the Wadi Rihadah az Zandi region (Figures 2 and 3B). The lack of a perfect correlation of the position of this zone with the exposed metagabbro suggests heterogeneity of the sources with depth. The causative sources should be related to the emplacement of intrusive rocks at depth.

The L1 negative zone is a lozenge–shaped area marked by a set of NE–SW oriented features (Figure 3B). Curves are superimposed with the eastern part of metagabbro of Jibal Jarfa, diorite–quartz diorite and older diorite in Wadi Daymaran and northward (Figures 2 and 3B). The zone L1 extends north–west up to UTM

y–coordinate 2190000N exhibiting a larger size of about 16 km in the Jibal as Saruf area. In the north–western part, the features overlie the metamorphic and volcano–sedimentary deposits of the Lif formation, and the intrusive rocks of Qirshah andesite, of older diorite and muscovite–quartz monzonite in the region of Jibal Ghuwayrah–Jabal Athrub–Jibal As Saruf (Figures 2 and 3B). The anomaly zone L1 is intersected by a relatively positive NE–SW feature and superimposed with the middle part of diorite in quartz diorite agmatite rocks of Jabal Zalma, and Qirshah Andesite and Muscovite Quartz Monzonite of the Jabal Bisharah region (Figures 2 and 3B). The L2 anomaly zone trends N–S and is composed of two NNE–trending main features of low intensity, associated with N– oriented other smaller anomalies (Figure 3B). This L2 zone overlies in large part intrusive rocks represented by older quartz diorite and older diorite, which covers the Al Mad–Suq Ithnayn domain (Figures 2 and 3B). The shape of the anomaly zone indicates a magnetization induced on rocks of low magnetic susceptibility compared to the adjacent rocks. Interestingly, the low magnetic signatures located at the western part of the area can be accounted for by unexposed structures at depth. Therefore, these zones appear to contain rocks of low magnetic susceptibility. The L3 anomaly zone in the central domain of the study area is represented by linear N– trending features to the North and changed towards the south–west to the South (Figure 3B). This zone located in the area where volcanosedimentary and metamorphic layers of the Ablah group belt (ar, ajb, at) are exposed (Figures 2 and 3B). A strong gradient corresponds to main lithological contrast between volcano–sedimentary layers and intrusive rocks and between the different groups of volcano–sedimentary and metamorphic rocks, which are affected by the Umm Farwah master fault zone (Figures 2 and 3B). The anomaly zone L4 is located at the northeastern end of the map (Figure 3B). This zone corresponds to a domain of Adimah ash Shamran–Al Wakabah that is marked mainly by outcropping of volcanosedimentary and metamorphic layers (jdq, jdk) of the Jiddah group (Figures 2 and 3B). The high gradient reflects the main lithological contrast between intrusive rocks to the west and volcano–sedimentary layers to the east (Figures 2 and 3B). These contacts are associated with major field faults, some of which are recognized within the same meta–sedimentary unit, the Jiddah group.

4.2 HORIZONTAL GRADIENT

The horizontal gradient magnitude (HGM) filter is an edge detection technique that was applied to the RTP data to allow determination of geological boundaries in

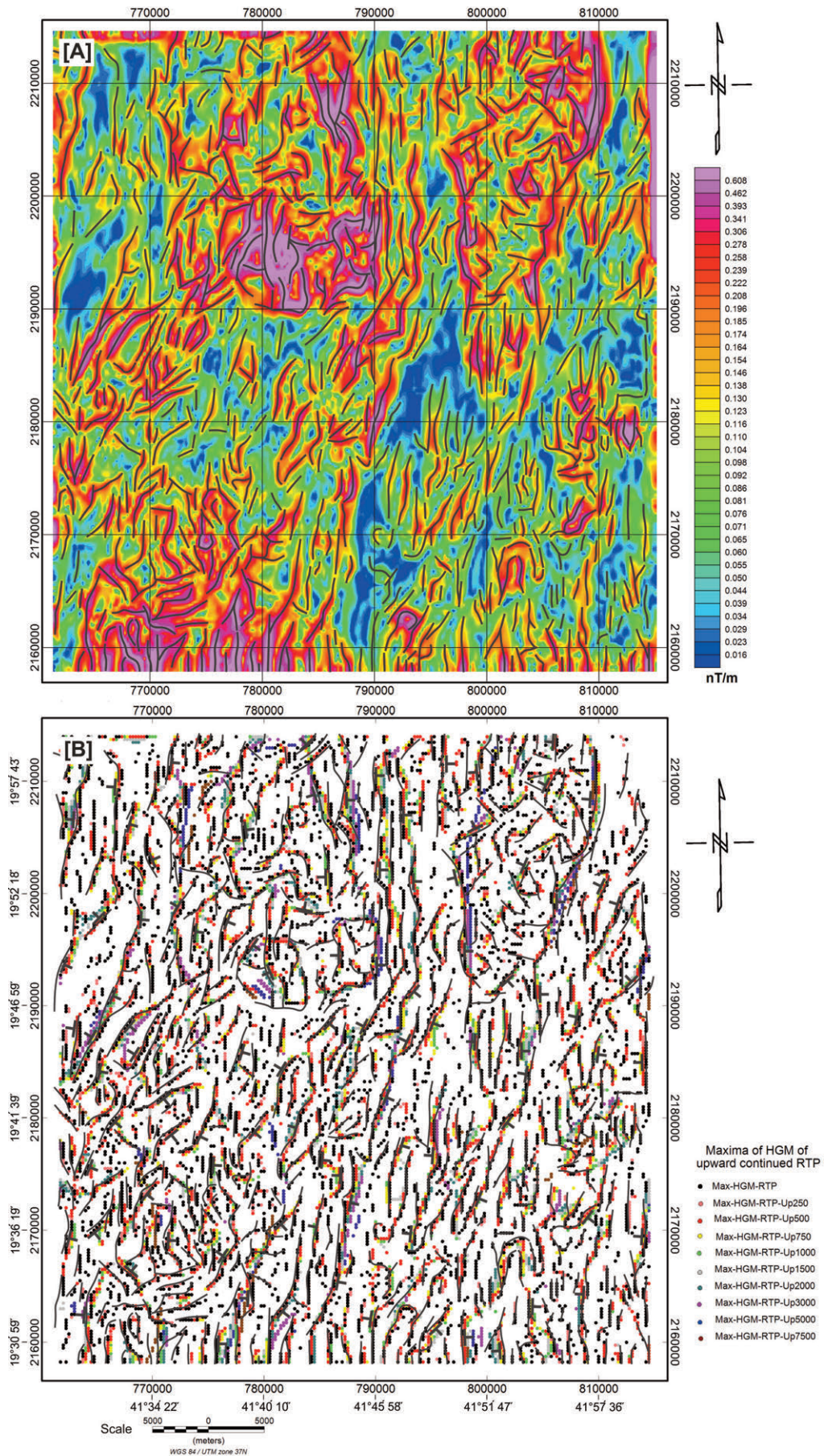


FIGURE 4. [A] Horizontal Gradient Magnitude (HGM) map of the Biljurshi study area and extracted lineaments. [B] Maxima of horizontal gradient magnitude (HGM) combined with the extracted lineaments, showing dip of the geologic contacts.

the Biljurshi region (Figure 4A). HGM gives an overview of the location of the magnetic contacts/faults.

The automatic identification of HGM maxima by scanning the data grid using movable window help identify the maxima at which faults occurred. Calculating the amplitude of the horizontal gradient for different elevations reveal horizontal offsets in the maxima (Figure 4B). The offsets may be interesting for geometrical characterization of the contact. If they are coherent along the same structure, these shifts can be interpreted as a dip (Figure 4B). The maximum of the amplitude of the horizontal gradient can be moved in the horizontal plane if the detected object has a dip. The solutions of maxima of the amplitudes of the horizontal gradient are aligned in different directions reflecting the location of the contacts.

Analysis of the direction of the interpreted sources shows that most contacts are aligned along an N-S orientation (Figure 4B). This study highlights structures with eastward and westward most dominant dips related to the N-S predominant structures. Other struc-

tures are not appeared to be affected by sufficient dips. This can be explained by vertical contacts which have contributed in rising of intrusive rocks.

4.3 3D EULER DECONVOLUTION

Depth estimation using Euler deconvolution method was applied for delineate geologic contacts. It provides automatic calculation of source location and depths. A depths map of contacts was calculated for the Biljurshi are using Euler deconvolution method (Figure 5). The parameters assigned for the obtained solutions, help us to define an optimal detection window of 4km * 4km according to the extent of the main anomaly zones. A structural index corresponding to magnetic contact (SI = 0) was chosen. The positions of the sources have been represented by colored circles whose sizes are proportional to the depth.

The 3D Euler deconvolution map illustrates aspects of the interpretation solutions of depth to magnetic sources (Figure 5). It shows that the area has a depths ranging from 100 m to 2800 m. The depth results help

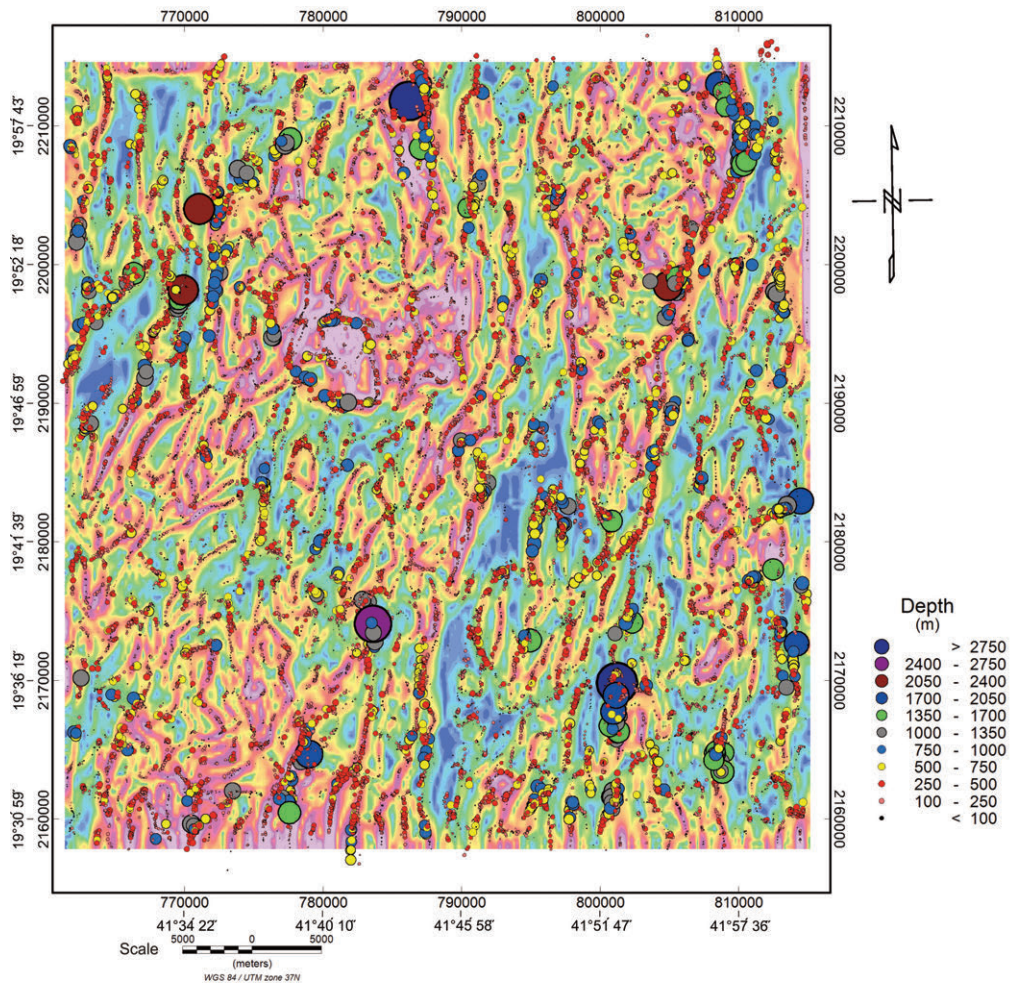


FIGURE 5. Euler solutions (SI =0) of RTP magnetic anomaly zone, showing estimated depth for highlighted geological contacts.

in interpretation of geological contacts of the buried magnetic structures. Numerous series of near surface contacts showed that the depth range, of near surface basement structures and contacts, is 500 to 1000 m (Figure 5). Meanwhile, the deep-seated basement structures and contacts are varying in depth between 1000 m and 2500 m. These near surface and deep-seated zones cut across and displace each other with different dislocations and directions. The depth solutions testify the geometrical and structural heterogeneity in depth.

Euler map is in agreement with the geological and structural framework as well as magnetic anomaly zones and lineaments. The characteristics of the Euler map reveal solutions with allures in concordance with the reduced to pole magnetic intensity, and the HGM maps (Figure 5).

4.4 FORWARD MODELING

To perform magnetic modeling, the AA' profile was extracted from the RTP magnetic intensity data (Figure 6A, B). It was chosen due to its crossing the strike of regional geological and geophysical trends (Figures 2 and 6B). The Biljurshi quadrangle is marked by the N-trending Ablah group belt associated with volcano-sedimentary and metamorphic layers, which are crossed by the Umm Farah master fault, and the intrusive plutonic and hypabyssal intrusive rocks that occupied the west and east parts. Therefore, transects were selected along the E-W direction to cross key lithologic contrasts and tectonic features.

The crustal model across the Ablah group belt and adjacent volcano-sedimentary and intrusive complex structures was constructed taking into account the local and regional tectonic framework. The cross-section extends more than 7 km below the surface (Figure 6B). The geometrical bodies in the cross section are estimated based on the exposed geological structures [Greenwood, 1975a]. To estimate the location and depth of the various magnetic anomalies along the selected profile, we used "Werner solutions" function that uses the horizontal and vertical derivatives. To facilitate imaging of shallow, intermediate and long sources, minimum and maximum window lengths used for Werner deconvolution are 400 and 7500. Two depth source models (Dike and contacts model) were assumed and their depths were estimated. Werner solutions generated by the dike model and the contact model reach maximum depths between 3000 m and 5000 m (Figure 6A); the RTP values varied from about -360 nT to +250 nT. These values are showed at the western part of the map and mainly coincide with the diorite intrusive rocks (Figure 6A, B). The magnetic model established along

profile AA' shows three different tectonic domains, the western accreted structures, the Ablah volcano-sedimentary dominated layers, and the eastern accreted structures (Figure 6B).

(i) The western domain, which shows a mixture of volcano sedimentary and metamorphic layers with intrusive rocks, occupies just under half of the line from the western border to the east of Marran-As Sufay area near UTM x-coordinate 786500E (Figures 2 and 6A, B). The deepest (≥ 3 km) and most abundant solution clusters are highlighted at the level of UTM x-coordinate about 768000E and 775000E at the borders of metagabbro intrusive structure of Jibal Jarfa, and at the level of UTM x-coordinate about 786250E at the western border of the Ablah group (Figures 2 and 6A, B). These levels, marked by peaks in the horizontal gradient magnitude (HGM) curve (Figure 6A) correspond to main lithological contrast between volcano-sedimentary layers and intrusive rocks and between two intrusive rocks as these observed at the Wadi Hazam (Figures 2 and 6A, B). Contacts are associated with major faults. The volcano-sedimentary and metamorphic layers are marked by low susceptibility ($k=0.002$) and thus, responsible for the negative magnetic anomaly (Figure 6B). Since intrusive rocks contain mafic minerals, high magnetic susceptibility was expected. Conversely, in our case, the metagabbro shows a negative anomaly of the reduced to pole total magnetic intensity curve (Figure 6B). The low variation in the anomaly is related to the magnetic susceptibility that could be variable based on the percentage of mafic minerals. However, the remarkable decrease of the magnetic value could be interpreted to be related to the limited vertical expansion of the matagabbro, which should corresponds to thin body located above the volcano-sedimentary layers of low magnetic susceptibility (Figure 6B). Nevertheless, some works [e.g., Ferraccioli et al., 2002] highlight to have ilmenite-rich gabbros too but are not highly magnetic at all.

(ii) The central domain corresponds to the Ablah group belt that extends, on the study section, from the east of Marran-As Sufay area near UTM x-coordinate close to 786500E to the west of Busaytah area near UTM x-coordinate close to 801750E (Figures 2 and 6A, B). This domain is marked by outcropping of the volcano-sedimentary and metamorphic layers of the Jiddah and Ablah groups, intruded by intrusive rocks of dioritic, serpentine and talc schist bodies (Figures 2 and 6A, B). The most abundant and deepest (more than 3500 m) solution clusters are highlighted at the level of UTM x-coordinate close to 790000E within Rafa Formation (ar), 794500E near the contact between the two Khutnah Formation (jdk) and Qirshah andesite (jqd) of the Jiddah group,

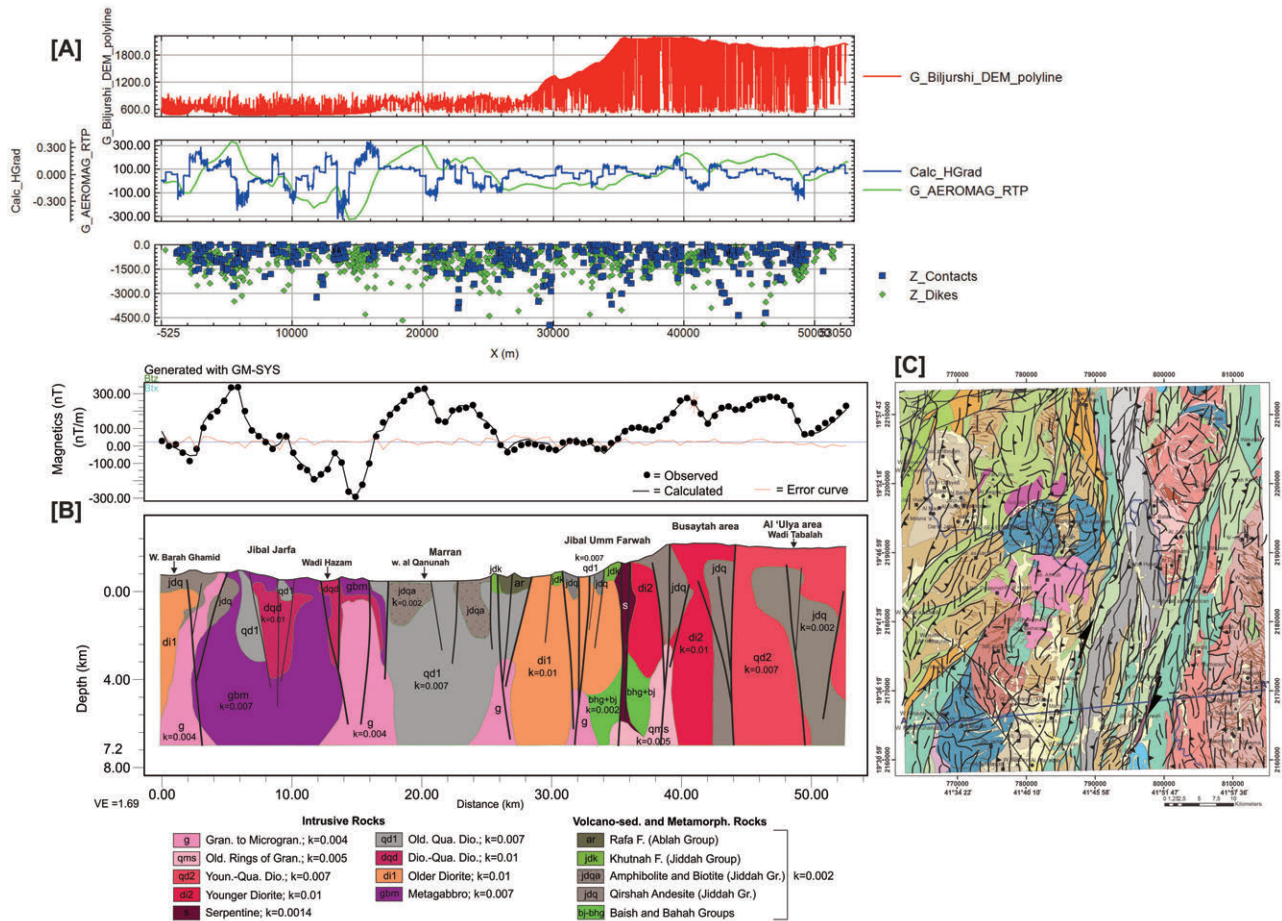


FIGURE 6. Interpreted geologic cross-section along the modeled profile AA. [A] Werner deconvolution solutions from a RTP magnetic intensity profile across the study area. From top to bottom, the sections correspond respectively to (i) the topography, (ii) the RTP profile (nT) with its HGM, and (iii) the contact and dike models in depth (m). [B] Modeled geological section, showing crossed basement bodies, and location of main faults based on the previous enhancements (HGM, Euler, and Werner). [C] Profile location on the deduced lineaments map; it is also given in figures 2 and 3.

798000E that coincides with the serpentine of Jibal Umm farwah, exposed between the two Khutnah Formation (jdk) and Qirshah andesite (jdq) of the Jiddah group, and 801750E near the contact between Qirshah andesite (jdq) of the Jiddah group and younger diorite (di2) (Figures 2 and 6A, B). The levels are marked by peaks in the HGM curve corresponding mainly to main lithological contrast between volcano-sedimentary layers and intrusive rocks and between the different groups of volcano-sedimentary and metamorphic rocks (Figures 2 and 6A, B). The contacts are associated with major faults forming the Umm Farwah shear zone (Figure 6B). This central domain is marked by low magnetic susceptibility, $k=0.0014$ for serpentine, and 0.002 for volcanic and metasedimentary rocks (Figure 6B). Low susceptibilities for the different bodies are required for the magnetic low anomalies. A series of magnetic highs and lows is interpreted to be formed by the magnetic susceptibility difference between volcano-sedimentary and intrusive rocks.

(iii) The eastern domain, extending from west of Busaytah area to the border, is marked by outcropping of intrusive rocks represented by younger diorite and younger quartz diorite (Figures 2 and 6A, B). In Werner solutions, the contact model, as compared to the dike model, shows most abundant and deepest solution clusters at the level of the UTM x-coordinate about 801750E near the contact between Qirshah andesite (jdq) of the Jiddah group and younger diorite (di2) of the Busaytah area, 806250E near the contact between younger diorite (di2) and younger quartz diorite (qd2) of Wadi Shaybanah, and 810750E at the level of Wadi Tabalah within the younger quartz diorite (qd2) of Al 'Ulya area (Figures 2 and 6A, B). These levels, marked by peaks in the horizontal gradient magnitude (HGM) curve, correspond to main lithological contrast between the two diorite and younger quartz diorite intrusive rocks. The contact is associated with a N-trending major exposed fault (Figures 2 and 6A, B). This eastern domain contains

dominant high magnetic anomalies with relatively low zones (Figure 6B). These responses indicate the prevalence of various intrusive rock units within the metasedimentary layers of the Jiddah group (Figure 6B).

4.5 INVERSION

In inversion, we consider that the remanent magnetization is negligible compared to the induced magnetization of the source. It will be limited only to solving of the inverse problem for the field magnetic data to obtain contrast of susceptibility. Otherwise, the inversion becomes more complicated because it must produce additional solutions to the inclination, declination and magnetization of the remanence. Without sufficient information about paleomagnetic data, we are not able to estimate the NRM contribution. So we inverted the data considering just the induced magnetic field [e.g., Williams, 2008, Cheyney et al., 2015].

A 3D inversion model of the study area was obtained using 3D VOXI tool of Oasis Montaj software. It shows spatial susceptibility contrast with depth (Figure 7). The obtained model reproduces the data with an average squared error between data and synthetic response of the model of about 10 nT (9.018 nT). The extracted inversion profile AA', which extends about 9000 m below ground, gives distribution of susceptibility contrast (Figure 7). The observed effect is probably also due to the high values of contrast related to surface units which, for unconstrained inversion, should mask by their intensities and effects of deeper sources. The output result model shows subvertical dips and seems to correspond to the exposed geological structures and main magnetic prints such as the intrusive bodies. Because of the extended scale of study area, some narrow geological structures and bodies, such as dykes, are not identified.

The intrusive structures in the eastern domain of the study area extend deeply and seem to have low dip either to the west or to the east related to the structural framework (Figure 7). The intrusions of the western domain are discontinuous with less width. The correlation with interfaces defined on the geological map should allow us to better restrict lateral and vertical extensions. Units interpreted as intrusive are fairly well identified with various continuities. However, it should be noted that field observations have shown that the gabbros could have different susceptibilities. The susceptibility may even vary greatly in the same body with several orders of magnitude, which could explain these discontinuities [Astic 2011]. The inversion has a tendency to group together certain magnetic units at depth despite considered as independent such as small

tight intrusions and synvolcanic dykes. Thus, the VOXI performs inversions that lead to individual source bodies of relatively low resolution.

5. DISCUSSION: TECTONIC FRAMEWORK

5.1 TECTONIC SIGNIFICANCE

Many geological structures (e.g., faults, folds, intrusions) can be highlighted using quantitative interpretation. All magnetic models and inversions combined together to provide information about the subsurface nature of the Biljurshi study area. The modeling and subsequent inversion shows that the deep structuring and geometry of the crust in Biljurshi is very complicated. Despite this structural complication, we have identified three different domains forming the study area with similar mostly N-S oriented structural fabric (Figure 8). The arrangements of the volcano-sedimentary and intrusive units demonstrate heterogeneity of deformation that seems to be linked to the inherited structural architecture, and then to the subsequent major constraints during accretion of the terranes.

The N-S direction, the most widespread in the entire region; is the main focus fault network in the Biljurshi area. Thus, these major faults represent the direction of tectonic boundaries, which have affected the region (Figure 8). A major part of the lineaments of N-S trend appears to be related to inherited faults affecting the basement of the Asir terrane. In the Ablah group domain, the N-S direction consists of volcano-sedimentary and metamorphic assemblages.

We realize the influence of near N-S regional structural trending of Asir terrane that composes the major part of the Arabian Shield. This terrane has been the subject of several tectonic and orogenic episodes followed by erosion that has shaped its morphology during the Precambrian times. In addition to these faults, associated with dykes and other intrusions of Precambrian age intersect the study area in all directions (N-S, NE-SW, NW-SE, and E-W). The structural framework testifies Precambrian tectonic deformations dominated by compressional stresses with joined local extensions that have controlled successive evolution of volcano-sedimentary and intrusive units in this part of the Arabian Shield. Kinematics and style of deformation were related to inherited tectonic deformations. Metasedimentary and volcanic series, and accreted igneous intrusions, were placed related to the pre-existing Neoproterozoic [Collins and Pisarevsky, 2005; Stern and Johnson, 2010; Johnson et al., 2011] prominent N-S cross-cutting faulting and structures.

AEROMAGNETIC CONSTRAINTS ON THE UMM FARWAH FAULT SYSTEM

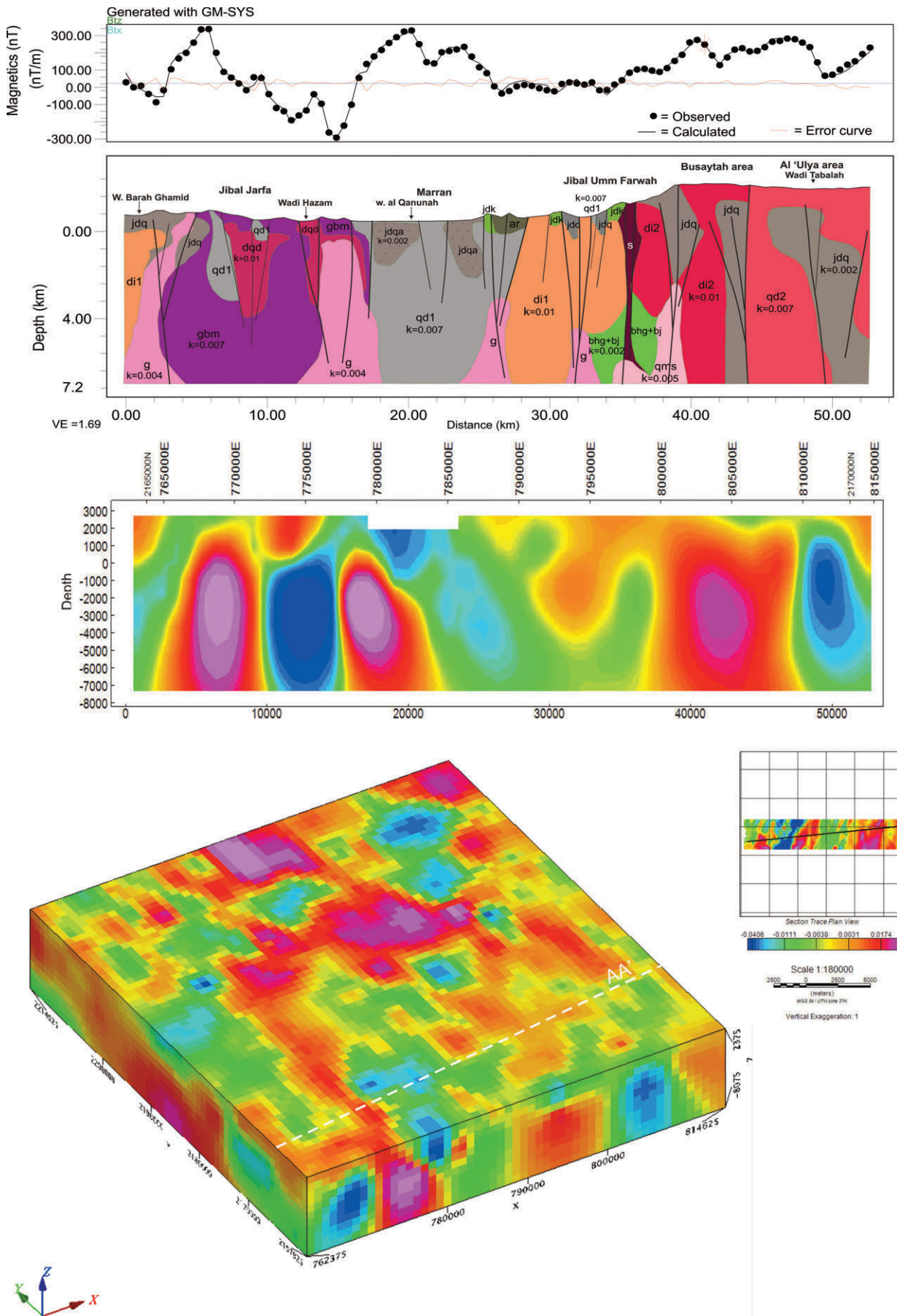


FIGURE 7. Inversion model of the study area, obtained from RTP magnetic data, showing the susceptibility contrast in depth. The inversion section AA', extracted from 3D inversion model obtained by 3D VOXI, is superimposed by the 2D forward model.

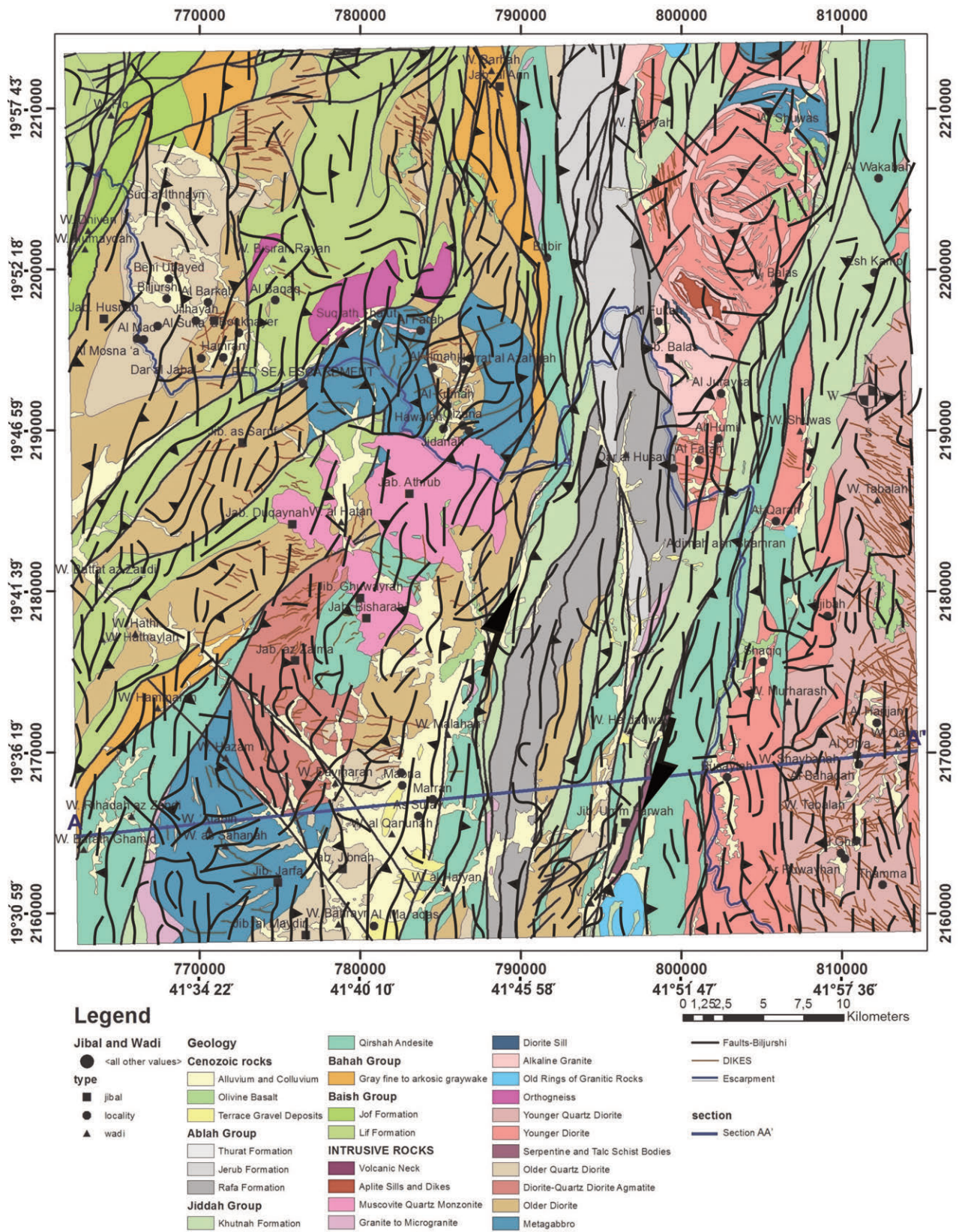


FIGURE 8. Interpreted structural setting of the Biljurshi area, showing the main deduced lineaments superimposed on the exposed geological map.

Faulting and subsurface change of crustal structuring in the Asir terrane are interpreted as characteristics of a syn-tectonic deformation within the same basement ter-

rane. Abrupt changes in crustal rocks testify high local fracturing and regional deformation. Geological structural and lithological patterns record major reverses struc-

tures indicating prominent contractional stresses that result in accretion phenomenon in the Asir terrane.

5.2 DEEP GEOMETRY AND STRUCTURING

Modeling locates the different sources in the crust and correlates with results suggested by the qualitative analysis of the magnetic anomalies. The susceptibility and shape parameters are not constrained. We can assume infinity of possibilities and the produced models are far from being unique; but they are the closest to the exposed geological structures.

Modeling and inversion along a transect in Biljurshi area suggest that the magnetic method can be useful tool in geological studies, such as estimate the location and deep geometries of dominant volcano-sedimentary and intrusive different domains forming the basement in the Arabian Shield. Location and deep geometry of faults, associated with the accretion deformation, are also quantified and highlighted. Some small structure of varied magnetic susceptibility should be also emphasized.

Although the detailed kinematic and origin of deposits of the Asir terrane is unclear, the boundary between the Ablah group domain and the adjacent accreted rocks to the west and east is clearly delineated in the models. A medium magnetic low, in the middle parts of the profile is interpreted to be caused by rocks of the Ablah group belt. This change in lithology of exposed rocks is related to tectonic inheritance that controlled sedimentary layout and kinematic belonging to the Asir terrane.

Results of magnetic modeling and inversion indicate that the crust of the Asir terrane is highly deformed (Figure 9) indicating that it has undergone successive major tectonics phases. This study reveals three domains that characterized the study area: dominated volcano-sedimentary and intrusive mixing to the west; dominated volcano-sedimentary domain at the center that is superimposed with the Ablah group belt; and dominated intrusive with volcano-sedimentary series to the east. Tectonic contact is the most identified feature; the highly fracturing is showed by the Umm Farwah shear zone.

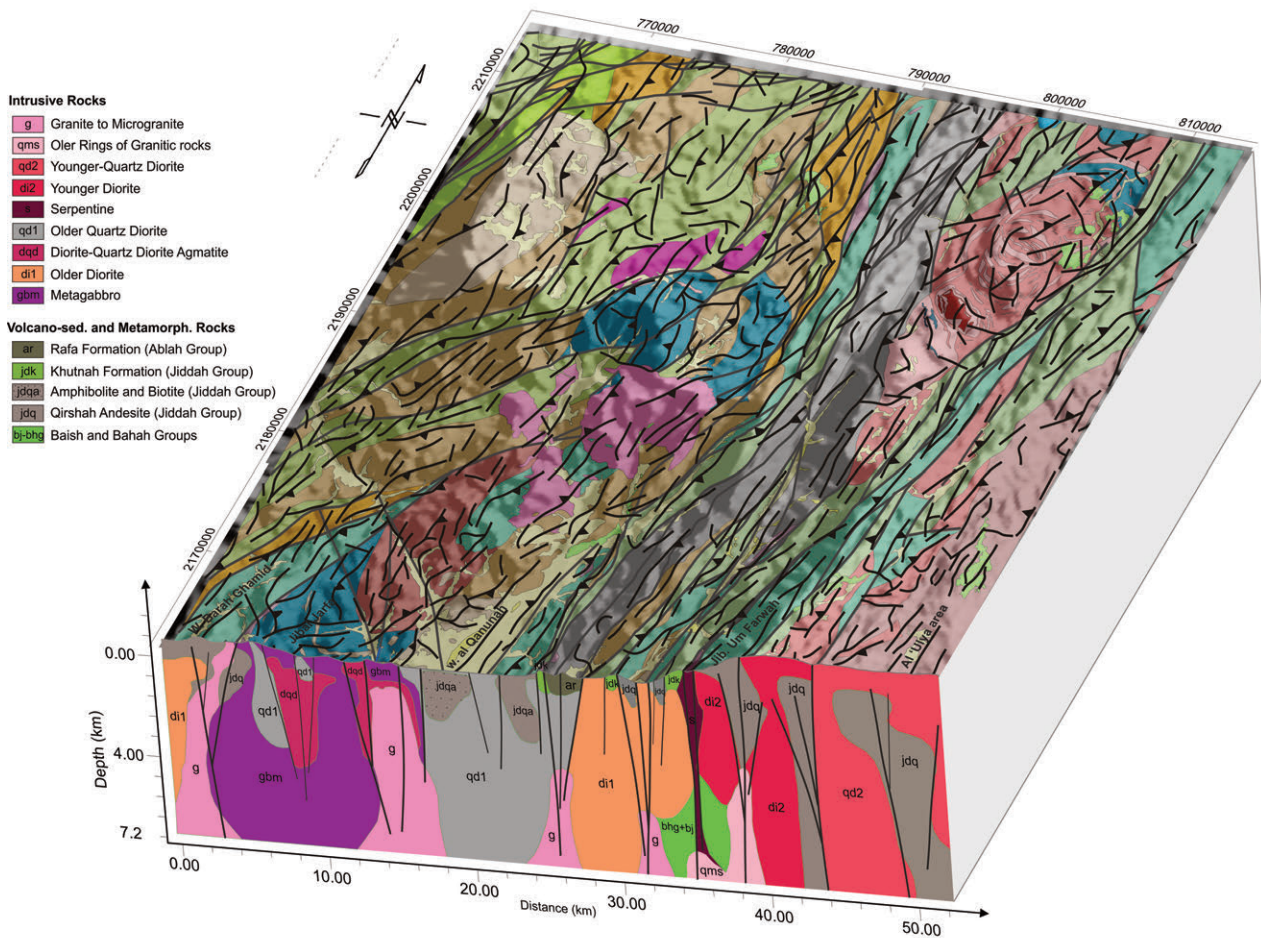


FIGURE 9. Block diagram 3D showing the structural framework and deep geometry of the volcano-sedimentary layers and intrusive bodies in the Biljurshi area.

The Umm Farwah shear zone, therefore, can be described as a distinct tectonic element in the magnetic model. Late Cryogenian–Ediacaran Assembly of the Gondwana supercontinent [Collins and Pisarevsky, 2005; Johnson, 2006; Johnson et al., 2011] has included convergence and compression of distant cratons. Movements along the Umm Farwah fault have induced subsiding domains between the separating intrusive dominated blocks, as syncline and/or graben system that were intruded by intrusive rocks, which extend along the major faults.

The magnetic anomalies correspond to signals that reflect the traces of ancient orogenic deformations and structures. These deformations would have induced a variation of the magnetic properties and thus differentiated fragments of crust from one another. Consequently, study of magnetic anomalies of the Biljurshi region seems to confirm the relationship between magnetic anomalies and the crustal zones already suggested previously in Asir terrane.

6. CONCLUSIONS

Analyses aeromagnetic data allowed us to characterize the tectonic framework and structural setting in the Biljurshi area. The geological structures were created during the Proterozoic major successive tectonic deformation phases and associated with regional metamorphism phenomena. The magnetic anomaly feature trends follow systematic orientations in response to regional stresses during the latest stages of ductile deformations.

The present study delineated new faults in the study area. Processing of aeromagnetic data was used for delineating geologic contacts and depth estimation, and consequently generated the structural map of the Biljurshi area. The various sets of structure locations were compiled to facilitate interpretation of the geological structures and associated deformations. Three major trends oriented nearly N-S (N-S, NNE-SSW and NNW-SSE) dominating the study area, the NE-SW direction is revealed in the central eastern part of the study area.

The present study highlights an excellent correlation between aeromagnetic features and lineaments, and exposed geological structures. The Biljurshi area was controlled by deep and regional tectonic stresses. The observed major faults crossing-out the study area seem to be superimposed on contact zones both between volcano-sedimentary and metamorphic layers and intrusive rocks, and between rocks of the same type (volcano-sedimentary or intrusive). This aspect shows

old features and of kinematics linked to the emplacement of the plutonic rocks and their contact with the volcano-sedimentary series. The N-oriented Umm Farwah deep major fault system, located at the location of the Ablah volcano-sedimentary group belt, could be ancient and has undergone later reactivations.

The integration of geophysical data with all available geological data, within a same 3D model, made it possible to constrain the geophysical models and inversions based on one or several geological scenarios. The comparison of the results with the other previous works, made it possible to make a geological link between the different elements. It is then possible to approved or modify some interpretations.

The current modeling and inversion highlighted a complex geological structure with varied extensions and depth. Considering the geological data, the whole Biljurshi area is interpreted as a part of Asir terrane, resulting from a complex and ancient evolution of the Arabian Shield. The 2D quantitative model shows that the study area is crossed by a N-S major deep faults, clearly visible on the surface. Sub-vertical dips indicate an E-W compressional stress. This fault corridor corresponds to the Umm Farwah famous fault, an ancient crustal fracture which has undergone phases of major successive deformations.

We established a refined map of lineaments and provide information on its origin as well as its geological and structural significance based on the spatial and deep behavior of the anomalies and lineaments (e.g., length, structure, orientation, density).

Acknowledgements. This project was funded by the Deanship of Scientific Research (DSR) at King Abdulaziz University, Jeddah, under grant no. G-367-145-37. The authors, therefore, acknowledge with thanks DSR for technical and financial support.

REFERENCES

- Al-Shanti, A.M.S (2009). The Geology of the Arabian Shield of Saudi Arabia. Scientific Publishing Center, King Abdulaziz University, Jeddah, Saudi Arabia, ISBN 978-9960-06-527-4, 190.
- Anderson, R.E. (1977). Geology of the Wadi Tarj Quadrangle, Sheet 19/42 A, Kingdom of Saudi Arabia. Saudi Arabian Directorate General of Mineral Resources (DGMR), Geologic Map GM-24, 24, Scale 1:100 000.
- Astic, T. (2011). Modélisation 3D et interprétation géologique du flanc nord du camp minier de Mata-

- gami par intégration de données et inversions géophysiques. Diplôme de Maîtrise ès sciences appliquées, génie minéral. École polytechnique de Montréal; Université de Montréal, 167.
- Bamoussa, A.O. (2013). Infracambrian superimposed tectonics in the Late Proterozoic units of Mount Ablah area, southern Asir Terrane, Arabian Shield, Saudi Arabia. *Arabian J. Geosci.*, 6, 2035–2044.
- Cheyney, S. (2012). 3D quantitative interpretation of archaeomagnetic surveys: application of mathematical modelling to determine depths and physical characteristics of buried materials. PhD Thesis, University of Leicester, England, UK, 310.
- Clark, D.A. and D.W. Emerson (1991). Notes on rock magnetization characteristics in applied geophysical studies. *Explor. Geophys.*, 22, 547–555.
- Collenette, P. and D.J. Grainger (1994). Mineral Resources of Saudi Arabia, not including Oil, Natural Gas, and Sulfur. Saudi Arabian Directorate General of Mineral Resources (DGMR), Special Publication, SP-2, 322.
- Collins, A.S. and S.A. Pisarevsky (2005). Amalgamating eastern Gondwana: The evolution of the circum-Indian orogens. *Earth-Science Rev.*, 71, 229–270.
- Ferraccioli, F., E. Bozzo and G. Capponi (2002). Aeromagnetic and gravity anomaly constraints for an early Paleozoic subduction system of Victoria Land, Antarctica. *Geophys. Res. Lett.*, 29 (10) 1406, doi: 10.1029/2001GL014138.
- Fleck, R.J., R.G. Coleman, H.R. Cornwall, W.R. Greenwood, D.G. Hadley, W.C. Prinz, J.S. Ratte and D.L. Schmidt (1973). Potassium-argon geochronology of the Arabian Shield. United States Geological Survey Saudi Arabian Project report, 165, 40, 15 figs.
- Fritz, H., M. Abdelsalam, K.A. Ali, B. Bingen, A.S. Collins, A.R. Fowler, W. Ghebreab, C.A. Hauzenberger, P.R. Johnson, T.M. Kusky, P. Macey, S. Muhongo, R.J. Stern and G. Viola (2013). Orogen styles in the East African Orogen: A review of the Neoproterozoic to Cambrian tectonic evolution. *J. Afr. Earth Sci.*, 86, 65–106.
- Genna, A., P. Nehlig, E. Le Goff, C. Guerrot and M. Shanti (2002). Proterozoic tectonism of the Arabian Shield. *Precambrian Research*, 117, 21–40.
- Goodwin, A.M. (1991). *Precambrian Geology*, Academic Press, London.
- Greenwood, W.R. (1975a). Geology of the Biljurshi quadrangle, sheet 19/41 B, Kingdom of Saudi Arabia; with a section on geophysical investigation, by G.E. Andreasen; geochemical investigation and mineral resources, by V.A. Trent and T.H. Kiilgaard. Saudi Arabian Directorate General of Mineral Resources (DGMR), Geologic Map GM-25, 31, scale 1:100 000.
- Greenwood, W.R. (1975b). Reconnaissance geology of the Jabal Shada quadrangle, sheet 19/41 A, Kingdom of Saudi Arabia. Saudi Arabian Directorate General of Mineral Resources (DGMR), Geologic Map GM-20, scale 1:100 000.
- Greenwood, W.R., R.E. Anderson, R.J. Fleck and R.J. Roberts (1980). Precambrian geologic history and plate-tectonic evolution of the Arabian shield: Saudi Arabian Directorate General of Mineral Resources Bulletin, 24, 35.
- Greenwood, W.R., D.B. Stoesser, R.J. Fleck and J.S. Stacey (1982). Late Proterozoic island-arc complexes and tectonic belts in the southern part of the Arabian shield, Kingdom of Saudi Arabia. Saudi Arabian Deputy Ministry for Mineral Resources, Open-File Report USGS-OF-02-8, 46.
- Greenwood, W.R., R.O. Jackson and P.R. Johnson (1986). Geologic map of the Jabal Al Hasir quadrangle, sheet 19F, Kingdom of Saudi Arabia. Saudi Arabian Deputy Ministry for Mineral Resources, Geoscience Map GM 94C, 31, scale 1:250 000.
- Hadley, D.G. (1975). Geology of the Wadi Hali quadrangle, sheet 18/41 B, Kingdom of Saudi Arabia, with a section on Aeromagnetic investigations, by G.E. Andreasen. Saudi Arabian Directorate General of Mineral Resources (DGMR), Geologic Map GM-21, 19 pp., scale 1:100 000.
- Hinze, W.J., R.R.B. Von Frese and A.H. Saad (2013). *Gravity and Magnetic Exploration: Principles, Practices, and Applications*. Cambridge University Press, Cambridge, ISBN 9780521871013, 512 pp.
- Hunt, C.P., B.M. Moskowitz and S.K. Banerjee (1995). Magnetic properties of Rocks and Minerals, in: *Rock Physics and Phase Relations – A hand book of Physical constants*, AGU Reference shelf 3, edited by: Ahrens, T. J., 189–204.
- Jacobs, J. and R.J. Thomas (2004). Himalayan-type indenter-escape tectonics model for the southern part of the late Neoproterozoic-early Paleozoic East African Antarctic orogen. *Geology* 32, 721–724.
- Jaques, A.L., P. Wellman, A. Whitaker and D. Wyborn (1997). High resolution geophysics in modern geological mapping. *J. Australian Geol. Geophys.*, 17 (2), 159–173.
- Johnson, P.R. (1998). The structural geology of the Samran-Shayban area, Kingdom of Saudi Arabia. Saudi Arabian Deputy Ministry for Mineral Resources

- sources, Open File Report USGS-OF-98-2, 45.
- Johnson, P.R. (2000). Proterozoic geology of western Saudi Arabia: Southern sheet. Saudi Geological Survey, Open-file Report SGS-OF-99-7, 48.
- Johnson, P.R. (2006). Explanatory notes to the map of Proterozoic geology of western Saudi Arabia. Saudi Geological Survey, Technical Report SGS, 62.
- Johnson, P.R., E. Scheibner and E. Alan Smith (1987). Basement fragments, accreted tectonostratigraphic terranes, and overlap sequences: Elements in the tectonic evolution of the Arabian Shield. In: Kröner, A. (ed.) Proterozoic lithospheric evolution. American Geophysical Union, Geodynamics Series, 17, 235-257.
- Johnson, P.R. and F.H. Kattan (2001). Oblique sinistral transpression in the Arabian shield: the timing and kinematics of a Neoproterozoic suture zone. *Precambrian Res.*, 107, 117-138.
- Johnson, P.R., F.H. Kattan and J.L. Wooden (2001). Implications of SHRIMP and microstructural data on the age and kinematics of shearing in the Asir terrane, southern Arabian shield, Saudi Arabia. *Gondwana Res.*, 4, 172-173.
- Johnson, P.R. and B. Woldehaimanot (2003). Development of the Arabian-Nubian Shield: perspectives on accretion and deformation in the northern East African Orogen and the assembly of Gondwana. Geological Society of London, Special Publication, 206, 289-325.
- Johnson, P.R., A. Andresen, A.S. Collins, A.R. Fowler, H. Fritz, W. Ghebreab, T. Kusky and R.J. Stern (2011). Late Cryogenian-Ediacaran history of the Arabian-Nubian Shield: A review of depositional, plutonic, structural, and tectonic events in the closing stages of the northern East African Orogen. *J. Afr. Earth Sci.*, 61, 167-232.
- Johnson, P.R., G.P. Halverson, T.M. Kusky, R.J. Stern and V. Pease (2013). Volcanosedimentary Basins in the Arabian-Nubian Shield: Markers of Repeated Exhumation and Denudation in a Neoproterozoic Accretionary Orogen. *Geosci. J.*, 3, 389-445.
- Ku, C.C. and J.A. Sharp (1983). Werner deconvolution for automated magnetic interpretation and its refinement using Marquart's inverse modeling. *Geophysics*, 48, 754-774.
- Meert, J.G. and B.S. Lieberman (2008). The Neoproterozoic assembly of Gondwana and its relationship to the Ediacaran-Cambrian radiation. *Gondwana Res.*, 15, 5-21.
- Moufti, M.R.H. (2001). Age, geochemistry, and origin of peraluminous A-type granitoids of the Ablah-Shuwas pluton, Ablah graben Arabian shield. *Acta Mineralogica-Petrographica*, Szeged, 42, 5-20.
- Muhongo, S., C. Hauzenberger and H. Sommer (2003). Vestiges of the Mesoproterozoic Events in the Neoproterozoic Mozambique Belt: The East African Perspective in the Rodinia Puzzle. *Gondwana Res.*, 6 (3), 409-416.
- Nehlig, P., A. Genna, F. Asfirane, N. Dubreuil, C. Guerrot, J.M. Eberlé, H.M. Kluyver, J.L. Lasserre, E. Le Goff, N. Nicol, N. Salpeteur, M. Shanti, D. Thiéblemont and C. Truffert (2002). A review of the Pan-African evolution of the Arabian Shield. *GeoArabia*, 7 (1), 103-124.
- Patchett, P.J. and C.G. Chase (2002). Role of transform continental margins in major crustal growth episodes. *Geology*, 30, 39-42.
- Porwal, A., E.J.M. Carranza and M. Hale (2006). Tectono-stratigraphy and base-metal mineralization controls, Aravalli province (western India): New interpretations from geophysical data analysis. *Ore Geol. Rev.*, 29 (3-4), 287-306.
- Prinz, W.C. (1975). Reconnaissance geology of the Jabal Aya quadrangle, sheet 18/42 A, Kingdom of Saudi Arabia, with a section on Aeromagnetic investigations, by G.E. Andreasen. Saudi Arabian Directorate General of Mineral Resources (DGMR), Geologic Map GM-17, 9, scale 1:100 000.
- Prinz, W.C. (1983). Geologic map of the Al Qunfudhah quadrangle, sheet 19E, kingdom of Saudi Arabia. Saudi Arabian Deputy Ministry for Mineral Resources, Geologic Map GM-70 C, 19, scale 1:250 000.
- Schetselaar, E.M. and J.J. Ryan (2009). Remote predictive mapping of the Boothia mainland area, Nunavut, Canada: an iterative approach using landsat ETM, aeromagnetic and geological field data. *Canadian J. Remote Sens.*, 35, S72-S94.
- Shackleton, R.M. (1986). Precambrian collision tectonics in Africa. In: Coward, M.P., and Ries, A.C. (eds.) *Collision Tectonics*. Geological Society, London, Special Publications, 19, 329-349.
- Shackleton, R.M. (1994). Review of Late Proterozoic sutures, ophiolitic melanges and tectonics of eastern Egypt and north-east Sudan. *Geol. Rundsch.*, 83, 537-546.
- Shackleton, R.M. (1996). The final collision zone between East and West Gondwana: Where is it?. *J. Afr. Earth Sci.*, 23, 271-287.
- Stern, R.J. (2002). Crustal evolution in the East African Orogen: A neodymium isotopic perspective. *J. Afr. Earth Sci.*, 34, 109-117.
- Stern, R.J. (1994). Arc assembly and continental collision in the Neoproterozoic East African Orogen: Implications for the consolidation of Gondwana-

- land. *Annu. Rev. Earth Pl. Sci.*, 22, 319–351.
- Stern, R.J. and P.R. Johnson (2010). Continental lithosphere of the Arabian Plate: A geologic, petrologic and geophysical synthesis. *Earth-Sci. Rev.*, 101, 29–67.
- Stoeser, D.B. and V.E. Camp (1985). Pan-African microplate accretion of the Arabian Shield. *Geol. Soc. Am. Bull.*, 96, 817–826.
- Stoeser, D.B. and J.S. Stacey (1988). Evolution, U-Pb geochronology and isotope geology of the Panafrican Nabitah orogenic belt of the Saudi Arabian Shield. In: El-Gaby, S. and R.O. Greiling (Eds.) *The Pan-African Belt of Northeast Africa and Adjacent Areas*. Vieweg, Braunschweig/Wiesbaden, 227–288.
- Williams, N.C. (2008). Geologically-constrained UBC-GIF gravity and magnetic inversions with examples from the Agnew-Wiluna greenstone belt, Western Australia. PhD Thesis, University of British Columbia, Available online from: <https://open.library.ubc.ca/cIRcle/collections/ubc-theses/24/items/1.0052390>.

*CORRESPONDING AUTHOR: Taher ZOUAGHI,
Geoexploration Department, Faculty of Earth Sciences,
King Abdulaziz University,
Jeddah 21589, Saudi Arabia;
email: tzouaghi@kau.edu.sa; taher.zouaghi2018@gmail.com

© 2019 the Istituto Nazionale di Geofisica e Vulcanologia.

All rights reserved